The proton and neutron distributions in Na isotopes: the development of halo and shell structure

J.Meng, I.Tanihata and S.Yamaji

The Institute of Physical and Chemical Research (RIKEN), Hirosawa 2-1, Wako-shi

Saitama 351-01, JAPAN

(February 6, 2008)

The interaction cross sections for ^{A}Na + ^{12}C reaction are calculated using Glauber model. The continuum Hartree-Bogoliubov theory has been generalized to treat the odd particle system and take the continuum into account. The theory reproduces the experimental result quite well. The matter distributions from the proton drip line to the neutron drip line in Na isotopes have been systematically studied and presented. The relation between the shell effects and the halos has been examined. The tail of the matter distribution shows a strong dependence on the shell structure. The neutron $N = 28$ closure shell fails to appear due to the coming down of the $2p_{3/2}$ and $2p_{1/2}$. The development of the halo was understood as changes in the occupation in the next shell or the sub-shell close to the continuum limit. The central proton density is found to be decreasing near the neutron drip line, which is due to the proton-neutron interaction. However the diffuseness of the proton density does not change for the whole Na isotopes.

PACS numbers : 21.10.Gv,21.60.-n,24.10.Cn,25.45.De

Key word: Relativistic mean field, pairing, continuum, halo,shell structure

The recent developments in the accelerator technology and the detection techniques all around the world have changed the nuclear physics scenario. It is now possible to produce and study the nuclei far away from the stability line – so called "EXOTIC NUCLEI". Experiments of this kind have casted new light on nuclear structure and novel and entirely unexpected features appeared: e.g. the neutron halo in ^{11}Li [1] and neutron skin [2] as the

rapid increase in the measured interaction cross-sections in the neutron-rich light nuclei. The extreme proton and neutron ratio of these nuclei and physics connected with these low density matter have attracted more and more attentions in nuclear physics as well as other fields such as astrophysics.

With the exotic matter distribution near the drip line, a lot of questions are still open, e.g., the relation between the halo and the shell effect , the difference about the proton and neutron distribution on the stability line and away from the stability line. How is the halo formed ? Are there a rapid change from the normal nuclear density to the halo density or a gradual change in the particle number ? As the matter distribution is not measurable directly , series of experiment at different incident beam energy are necessary in order to determine the density distribution of both proton and neutron model-independently. Among all the experiments carried out so far, Na isotopes provide a good opportunity to study the density distributions over a wide range of neutron numbers [3]. Although theoretically, lots of works have been reported with either the non-relativistic Hartree-Fock or relativistic mean field, but the pairing property is always neglected or simply treated by the BCS approximation, e.g., see [4], [5]. For the pairing correlation, the contribution from the continuum are essential for the description of the drip line nuclei. We report in this letter a systematic study of nuclear density distributions in Na isotopes within the Relativistic Mean Field Theory (RMF), with the pairing and the blocking effect for odd particle system properly described by Hartree-Bogoliubov theory in coordinate representation, and try to answer some of the general questions in these low-density nuclear matter.

Definitely it is necessary to have a self-consistent theory to describe directly the cross section, so that the usual model dependent way for extracting the matter distribution could be avoided. As discussed in great detail in a recent review article [6] and in the references given therein, one has applied so far rather different techniques to describe halo phenomena in light nuclei, as for instance the exact solution of few-body equations treating inert sub-clusters as point particles, or the density dependent Hartree-Fock method in a localized mean field taking into account all the particles in a microscopic way, or a full shell model

diagonalizations based on oscillator spaces with two different oscillator parameters for the core- and the halo-particles. Recently, a fully self-consistent calculation within the Relativistic Hartree-Bogoliubov (RHB) theory in coordinate space for the description of the chain of Lithium isotopes ranging from ^{6}Li to ^{11}Li was reported [7]. It combines the advantages of a proper description of the spin-orbit term with those of full Hartree-Bogoliubov theory in the continuum, which allows in the canonical basis the scattering of Cooper pairs to low lying resonances in the continuum. Excellent agreement including binding energy, matter radius, and matter distribution with the experimental data was obtained without any modification of the neutron $1p_{1/2}$ level like the former works (see [7] and the references therein).

We first study the isospin dependence of the density distribution and the ground state properties of the Na nuclei within RHB. Then the cross sections based on Glauber model calculations with the density obtained from RHB are directly compared with the experimentally determined ones. As the theory used here is fully microscopic and parameter free, it gives consistent description of the proton and neutron distribution, and the development of proton and neutron halo or skin could be examined.

The basic ansatz of the RMF theory is a Lagrangian density whereby nucleons are described as Dirac particles which interact via the exchange of various mesons and the photon. The mesons considered are the scalar sigma (σ), vector omega (ω) and iso-vector vector rho (ρ). The latter provides the necessary isospin asymmetry [8]. The scalar sigma meson moves in a self-interacting field having cubic and quartic terms with strengths g_2 and g_3 respectively. The Lagrangian then consists of the free baryon and meson parts and the interaction part with minimal coupling, together with the nucleon mass M and m_σ (g_σ), m_ω (g_ω) and m_ρ (g_ρ) the masses (coupling constants) of the respective mesons:

$$\begin{aligned}\mathcal{L} &= \bar{\psi}(i\partial\!\!\!/ - M)\psi + \tfrac{1}{2}\partial_\mu\sigma\partial^\mu\sigma - U(\sigma) - \tfrac{1}{4}\Omega_{\mu\nu}\Omega^{\mu\nu} \\ &+\tfrac{1}{2}m_\omega^2\omega_\mu\omega^\mu - \tfrac{1}{4}\vec{R}_{\mu\nu}\vec{R}^{\mu\nu} + \tfrac{1}{2}m_\rho^2\vec{\rho}_\mu\vec{\rho}^\mu - \tfrac{1}{4}F_{\mu\nu}F^{\mu\nu} \\ &-g_\sigma\bar{\psi}\sigma\psi \;-\; g_\omega\bar{\psi}\omega\!\!\!/\psi \;-\; g_\rho\bar{\psi}\vec{\rho}\!\!\!/\vec{\tau}\psi - \; e\bar{\psi}A\!\!\!/\psi\end{aligned} \tag{1}$$

where a non-linear scalar self-interaction $U(\sigma)$ of the σ meson has been taken into account

[9].

For the proper treatment of the pairing correlations and for correct description of the scattering of Cooper pairs into the continuum in a self-consistent way, one needs to extend the present relativistic mean-field theory to a continuum RHB theory [10]. Using Green's function techniques it has been shown in Ref. [11] how to derive the RHB equations from such a Lagrangian:

$$\begin{pmatrix} h & \Delta \\ -\Delta^* & -h^* \end{pmatrix} \begin{pmatrix} U \\ V \end{pmatrix}_k = E_k \begin{pmatrix} U \\ V \end{pmatrix}_k , \tag{2}$$

E_k are quasi-particle energies and the coefficients $U_k(r)$ and $V_k(r)$ are four-dimensional Dirac spinors. h is the usual Dirac Hamiltonian

$$h \;=\; \boldsymbol{\alpha p} \;+\; g_\omega \omega \;+\; \beta(M + g_\sigma \sigma) \;-\; \lambda \tag{3}$$

containing the chemical potential λ adjusted to the proper particle number and the meson fields σ and ω determined as usual in a self-consistent way from the Klein Gordon equations in *no-sea*-approximation.

The pairing potential Δ in Eq. (2) is given by

$$\Delta_{ab} \;=\; \frac{1}{2} \sum_{cd} V^{pp}_{abcd} \kappa_{cd} \tag{4}$$

It is obtained from the pairing tensor $\kappa = U^* V^T$ and the one-meson exchange interaction V^{pp}_{abcd} in the pp-channel. As in Ref. [7] V^{pp}_{abcd} in Eq. (4) is the density dependent two-body force of zero range:

$$V(\boldsymbol{r}_1, \boldsymbol{r}_2) \;=\; \frac{V_0}{2}(1 + P^\sigma)\delta(\boldsymbol{r}_1 - \boldsymbol{r}_2)\,(1 - \rho(r)/\rho_0)\,. \tag{5}$$

The RHB equations (2) for zero range pairing forces are a set of four coupled differential equations for the HB quasi-particle Dirac spinors $U(r)$ and $V(r)$. They are solved by the shooting method in a self-consistent way as [7]. With a step size of 0.1 fm and using proper boundary conditions the above equations are solved in a spherical box of radius $R = 25$ fm. As shown in [12], for these relatively lighter nuclei $R = 25$ fm give quite accurate result.

Since we use a pairing force of zero range (5) we have to limit the number of continuum levels by a cut-off energy. For each spin-parity channel 20 radial wave functions are taken into account, which corresponds roughly to a cut-off energy of 120 MeV for $R = 25$. After fixing the cut-off energy and the box radius R, the strength V_0 of the pairing force (5) for both the neutrons and protons is fixed by a similar calculation of Gogny force D1S [13] by reproducing the corresponding pairing energy $-\frac{1}{2}\mathrm{Tr}\Delta\kappa$i as ref. [7]. For ρ_0 we use the nuclear matter density 0.152 fm^{-3}. The ground state $|\Psi>$ of the even particle system is defined as the vacuum with respect to the quasi-particle: $\beta_\nu|\Psi>= 0$, $|\Psi>= \prod_\nu \beta_\nu|->$, where $|->$ is the bare vacuum. For odd system, the ground state can be correspondingly written as: $|\Psi>_\mu = \beta_\mu^\dagger \prod_{\nu\neq\mu} \beta_\nu|->$, where μ is the level which is blocked. The exchange of the quasiparticle creation operator $\beta_\mu^\dagger$ with the corresponding annihilation operator β_μ means the replacement of the column μ in the U and V matrices by the corresponding column in the matrices V^*, U^* [15].

A systematic set of calculations have been carried out for all the nuclei in Na isotopes with mass number A ranging from 17 to 45. We have employed in the calculations the non-linear Lagrangian parameter set NLSH which was widely used for the description of all the medium and heavy nuclei, particularly drip line nuclei [16].

The calculated binding energies E_B and the interaction cross sections with the Glauber Model are presented in Figure 1. The calculated binding energies E_B are in good agreement with the empirical values [17] for the radioactive isotopes, which are our current interests. The resonance states of ^{17}Na and ^{18}Na (with a positive Fermi energy) are exactly reproduced. ^{19}Na is bound but unstable against the proton emission, reproducing the experimental observation. The neutron drip-line nucleus has been predicted to be ^{45}Na in the present model. The difference between the calculations and the empirical values for the stable isotopes is from the deformation, which has been neglected here.

To compare the cross section directly with experimental measured values, the densities $\rho_{n,p}(r)$ of the target ^{12}C and the Na isotopes obtained from RHB (see Fig.2) were used. The cross sections were calculated in Glauber model by using the free nucleon-nucleon cross

section [14] for the proton and neutron respectively. The cross sections for reaction of Na isotopes at 950A MeV on ^{12}C have been compared with the experimental values [3] in the upper part of Fig.1. The agreement between the calculated results and measured ones are fine. The cross section below ^{22}Na changes only slightly with the neutron number, which means the proton density has played important role to remedy the contribution of less neutron. From ^{25}Na to the neutron drip line, a gradual increase of the cross section has been observed. After ^{32}Na, although no data exist yet, a relatively fast increase has been predicted. As we have seen here, the measured cross section shows similar behavior with that of RHB.

As the density, which is obtained from a fully microscopic and parameter free model, is well supported by the experimental cross sections and binding energies, we proceed to examine the density distributions of the whole isotopes and study the relation between the development of halo and shell effect within the model.

The density distributions for both the proton and the neutron are given in Fig.2 . As seen in the upper part of Fig.2 , the change of the neutron density is as follows: for the nucleus with less number of neutrons (N), the density at the center is low and it spreads only to some smaller distance. With the increase of N, the density near the center increases due to the occupation of the $2s_{1/2}$ level, so does the development of neutron radius. In the lower part of Fig.2 , the proton density shows different behavior. The surface is more or less unchanged because of the Coulomb Barrier, but with the increase of N, the density of the center decreases due to the slight increasing at the tail. This is considered to be due to the attractive proton neutron interaction. But as the density must be multiplied by a factor $4\pi r^2$ before the integration in order to give the fixed Z, the big change in the center does not influence the outer part of the proton distribution very much. This result is fully consistent with the recent experiment on the charge-changing cross section [18].

The matter densities for the even N Na isotopes are given in Fig.3. the shortest tail in the total density occurs for $^{23-25}$Na, the most stable ones. For either the proton or the neutron rich side, the tail density increases monotonically. The tail ($r > 10$ fm) of the

proton rich nuclei is mainly due to the contribution of the proton and that of the neutron drip-line is mainly due to the contribution of the neutron. Compared with the neutron-rich isotopes, the proton distribution with less N has higher density at the center, lower density in the middle ($2.5 < r < 4.5$fm), a larger tail in the outer ($r > 4.5$ fm) part.

Next we will examine the density distribution for the neutron rich side. It is interesting to connect the matter distribution with the level distribution (See Fig.4): after ^{25}Na, as it is a sub-closure shell for the $1d_{5/2}$, then the neutrons are filled in the $2s_{1/2}$ and $1d_{3/2}$. So the tail of the density for ^{27}Na is two order of magnitude larger than ^{25}Na at $r = 10$ fm, while the tail of the density from ^{27}Na to ^{31}Na is very close to each other. But as more neutrons are filled in, the added neutrons are filled in the next shell $1f_{7/2}$, $2p_{3/2}$ and $2p_{1/2}$. So again two order of magnitude's increase has been seen from ^{31}Na to ^{33}Na, and then a gradual increase after ^{33}Na. So it becomes clear that the rapid increase in the cross section is connected with the filling of neutrons in the next shell or sub shell. In the inserts in Fig.3 : the radius r_0 at which $\rho(r_0) = 10^{-4}$ fm^{-3} is given as a function of the mass number to see the relation between the shell effect and matter distribution more clearly. It is very interesting to see a slight decrease of r_0 from proton drip-line to ^{25}Na. The tail of ^{25}Na is the smallest. From ^{26}Na to ^{31}Na, one sees a almost constant r_0. After a jump from ^{31}Na to ^{32}Na, a rapid increasing tendency appears again.

In Figures 4 , the microscopic structure of the single particle energies in the canonical basis [15] is given. In the left panel of Fig. 4, the single particle levels in the canonical basis for the isotopes with an even neutron number are shown. Going from $A = 19$ to $A = 45$ we observe a big gap above the $N = 8$, $N = 20$ major shell , and $N = 14$ sub-shell. The $N = 28$ shell for stable nuclei fails to appear, as the $2p_{3/2}$ and $2p_{1/2}$ come so close to $1f_{7/2}$. When $N \geq 20$, the neutrons are filled to the levels in the continuum or weakly bound states in the order of $1f_{7/2}$, $2p_{3/2}$, $2p_{1/2}$, and $1f_{5/2}$. In the right part, the occupation probabilities in the canonical basis of all the neutron levels below $E = 10$ MeV have been given for ^{35}Na to show how the levels are filled in nuclei near the drip line. The importances of careful treatment of the pairing correlation, of treating properly the scattering of particle pairs to

higher lying levels, are noted in the figure.

Summarizing our investigations, the development of a proton skin as well as neutron skin has been systematically studied with a microscopic RHB model, where the pairing and blocking effect have been treated self-consistently. A systematic set of calculations for the ground state properties of nuclei in Na isotopes is presented using the RHB together with standard Glauber theory. The RHB equations are solved self-consistently in coordinate space so that the continuum and the pairing have been better treated. The calculated binding energies are in good agreement with the experimental values. A Glauber model calculation has been carried out with the density obtained from RHB. A good agreement has been obtained with the measured cross sections for ^{12}C as a target and a rapid increase of the cross sections has been predicted for neutron rich Na isotopes beyond ^{32}Na. The systematics of the proton and neutron distribution are presented. After systematic examination of the neutron, proton and matter distributions in the Na nuclei from the proton drip-line to the neutron drip-line, the connection between the tail part of the density and the shell structure has been found. The tail of the matter distribution is not so sensitive to how many particles are filled in a major shell. Instead it is very sensitive to whether this shell has occupation or not. The physics behind the skin and halo has been revealed as a spatial demonstration of shell effect: simply the extra neutrons are filled in the next shell and sub-shell. This is in agreement with the mechanism observed so far in the halo system but more general. As the $1f_{7/2}$ is very close to the continuum, the $N = 28$ close shell for stable nuclei fails to appear due to the coming down of the $2p_{3/2}$ and $2p_{1/2}$ levels. Another important conclusion here is that, contrary to the usual impression, the proton density distribution is less sensitive to the proton and neutron ratio. Instead it is almost unchanged from the proton drip-line to the neutron drip-line. Similar conclusion has been obtained recently by charge change reaction experimently [18]. The influence of the deformation, which is neglected in the present investigation, is also interesting to us, more extensive study by extending the present study to deformed cases are in progress

[1] I.Tanihata et al, Phys.Rev.Lett. **55** (1985) 2676
I.Tanihata, Prog.Part.and Nucl.Phys.,**35** (1995) 505

[2] G.D.Alkhazov et al, Phys.Rev.Let. **78** (1997) 2313

[3] T.Suzuki et al, Phys.Rev.Let. **75** (1995) 3241

[4] X.Campi, et al, Nucl.Phys., **A251** (1975) 193

[5] S.Patra, and C.Praharaj, Phys.Let. **B273** (1991) 13

[6] M.V.Zhukov et al, Phys.Rep. **231** (1993) 150

[7] J.Meng, and P.Ring, Phys.Rev.Lett. **77** (1996) 3963

[8] P. Ring, Prog.Part. and Nucl.Phys. **37** (1996) 193.

[9] J.Boguta, and A.R.Bodmer, Nucl.Phys. **A292** (1977) 413

[10] J.Dobaczewski, H.Flocard and J.Treiner, Nucl.Phys. **A422** (1984) 103.

[11] H.Kucharek and P.Ring, Z.Phys. **A339** (1991) 23

[12] J.Meng, and P.Ring, Phys.Rev.Lett. (**to appear**)

[13] J.F.Berger, M.Girod, and D.Gogny, Nucl.Phys. **A428** (1984) 32c

[14] L.Ray, Phys.Rev.**C** 20 (1979) 1857

[15] P.Ring and P.Schuck, *The Nuclear Many-body Problem*, Springer Verlag, Heidelberg (1980)

[16] M.Sharma, M.Nagarajan and P.Ring, Phys.Lett. **B312** (1993) 377

[17] G.Audi, and A.H.Wapstra, Nucl.Phys. **A565** (1993) 1

[18] O.Bochkarev, et al, *submitted to* Z.Phys.

Figure Captions

Fig. 1 Upper part: The interaction cross sections σ_I of ^{A}Na isotopes on a carbon target at $950A$ MeV: the open circles are the result of RHB and the available experimental data ($A = 20 - 23, 25 - 32$) are given by solid circles with their error-bar. The dashed line is a simple extrapolation based on the RHB calculation for $^{28-31}$Na. Lower part: Binding energies for Na isotopes, the convention is the same as the upper part, but the RHB result for particle unstable isotopes are indicated by triangle.

Fig. 2 The neutron (upper) and proton (lower) density distributions in Na isotopes. The same figures but in logarithm scale are given as inserts to show the tail part of the density distribution.

Fig. 3 The same as Fig.2 but for matter density distribution. The upper part is given in logarithm scale (the radius is labeled at the top of the figure) and the radius r_0 at which $\rho(r_0) = 10^{-4}$ for different isotopes is given as inserts.

Fig. 4 Left part: Single particle energies for neutrons in the canonical basis as a function of the mass number. The dashed line indicates the chemical potential. Right part: The occupation probabilities in the canonical basis for ^{35}Na.

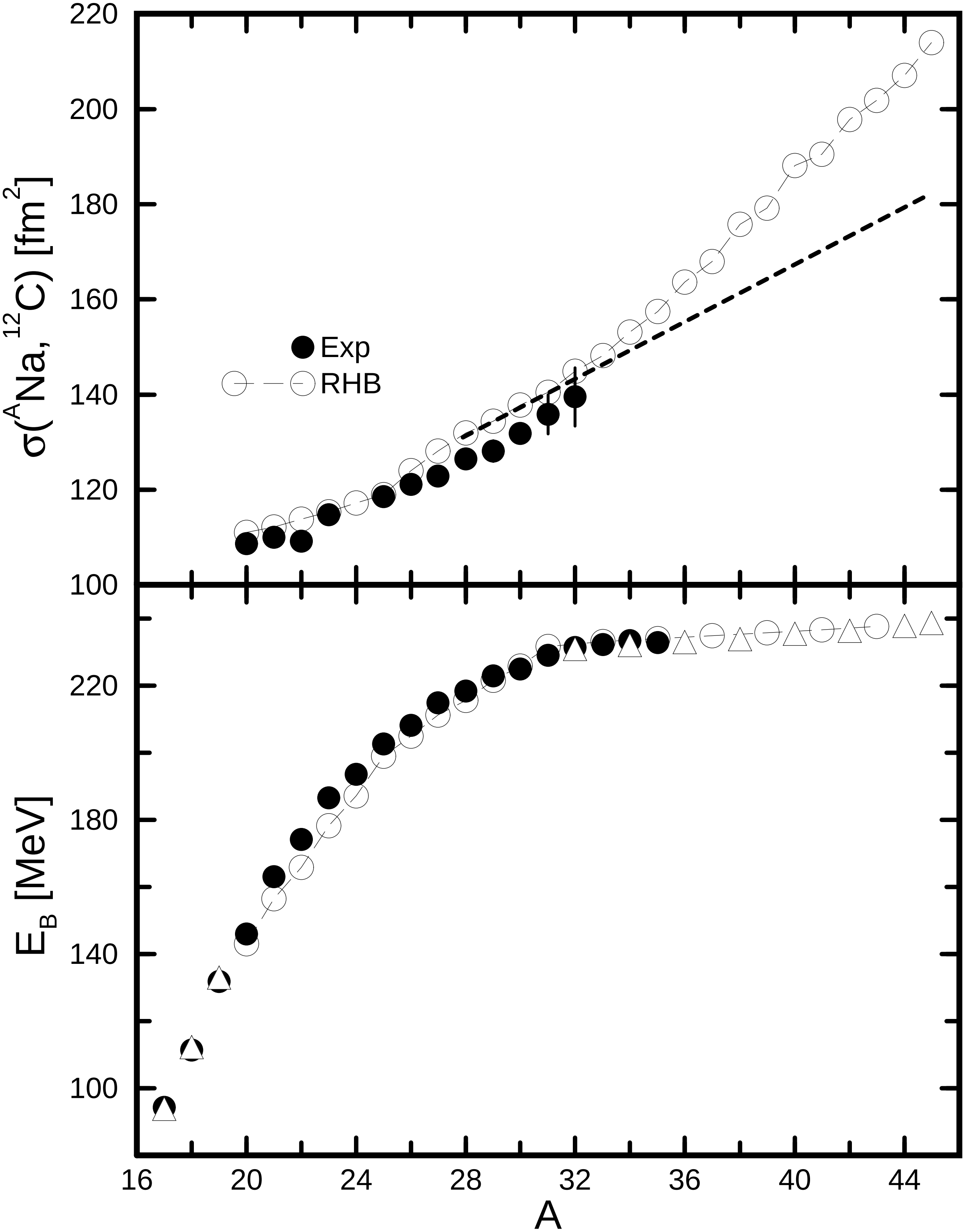
σ(^{A}Na, ^{12}C) [fm^{2}]
Exp
RHB
E$_B$ [MeV]
A
220
200
180
160
140
120
100
220
180
140
100
16
20
24
28
32
36
40
44

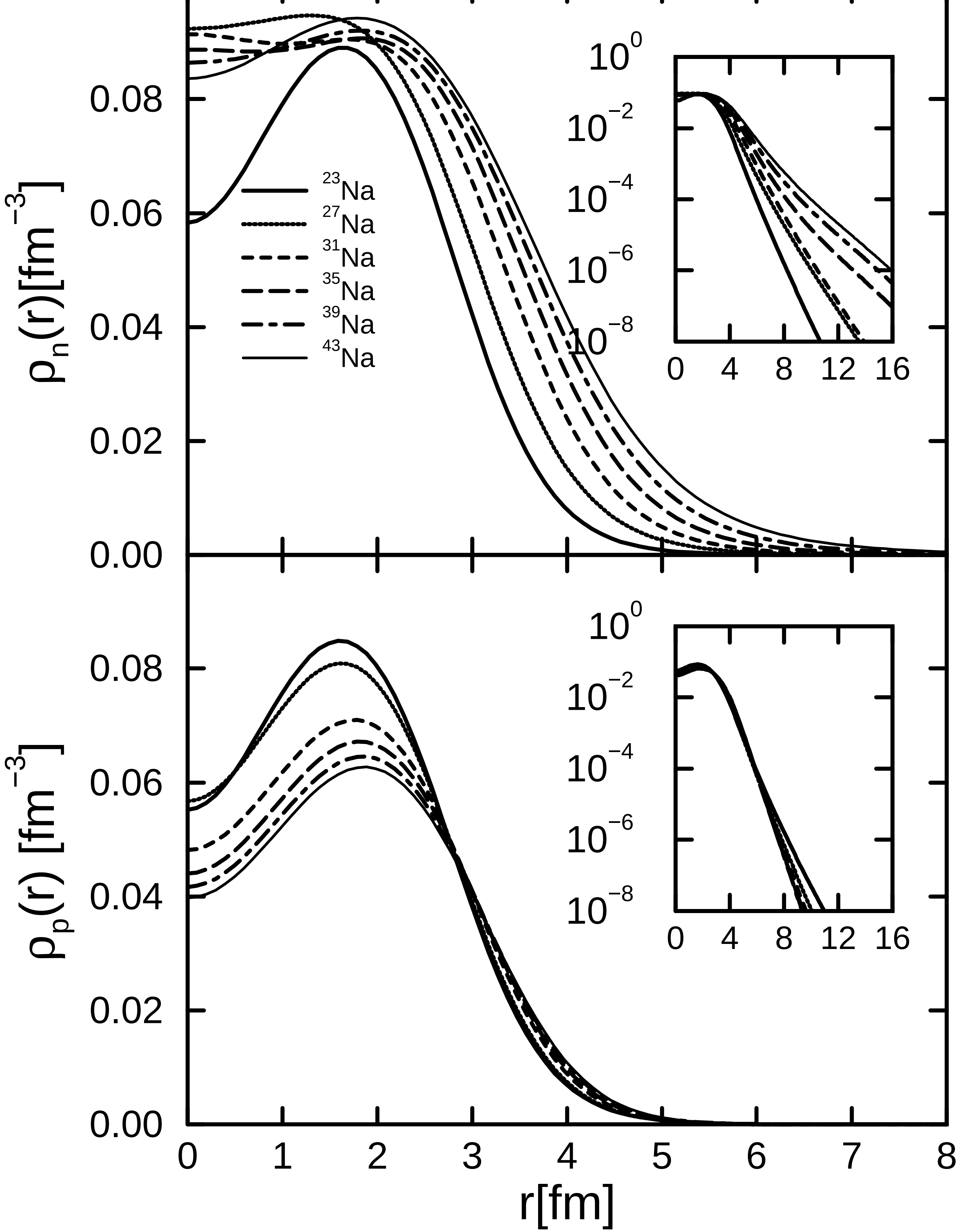

0.00
0.02
0.04
0.06
0.08
$\rho_n(r)[fm^{-3}]$
^{23}Na
^{27}Na
^{31}Na
^{35}Na
^{39}Na
^{43}Na
10^0
10^{-2}
10^{-4}
10^{-6}
10^{-8}
0 4 8 12 16
$\rho_p(r)$ $[fm^{-3}]$
0 1 2 3 4 5 6 7 8
r[fm]

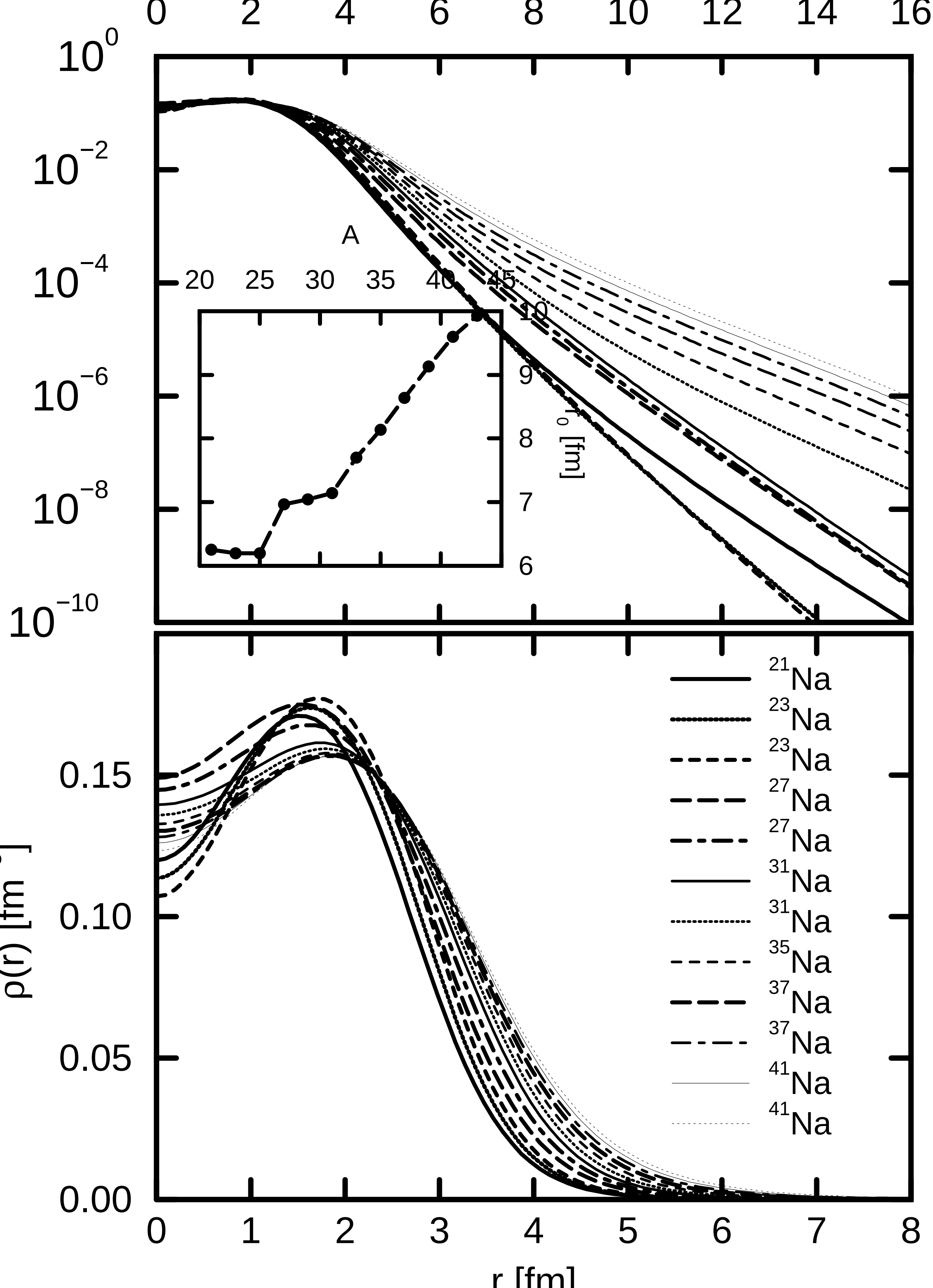

0
2
4
6
8
10
12
14
16
10^0
10^{-2}
10^{-4}
10^{-6}
10^{-8}
10^{-10}
A
20
25
30
35
40
45
10
9
8
7
6
r_0 [fm]
0.15
0.10
0.05
0.00
$\rho(r)$ [fm^{-3}]
0
1
2
3
4
5
6
7
8
r [fm]
^{21}Na
^{23}Na
^{23}Na
^{27}Na
^{27}Na
^{31}Na
^{31}Na
^{35}Na
^{37}Na
^{37}Na
^{41}Na
^{41}Na

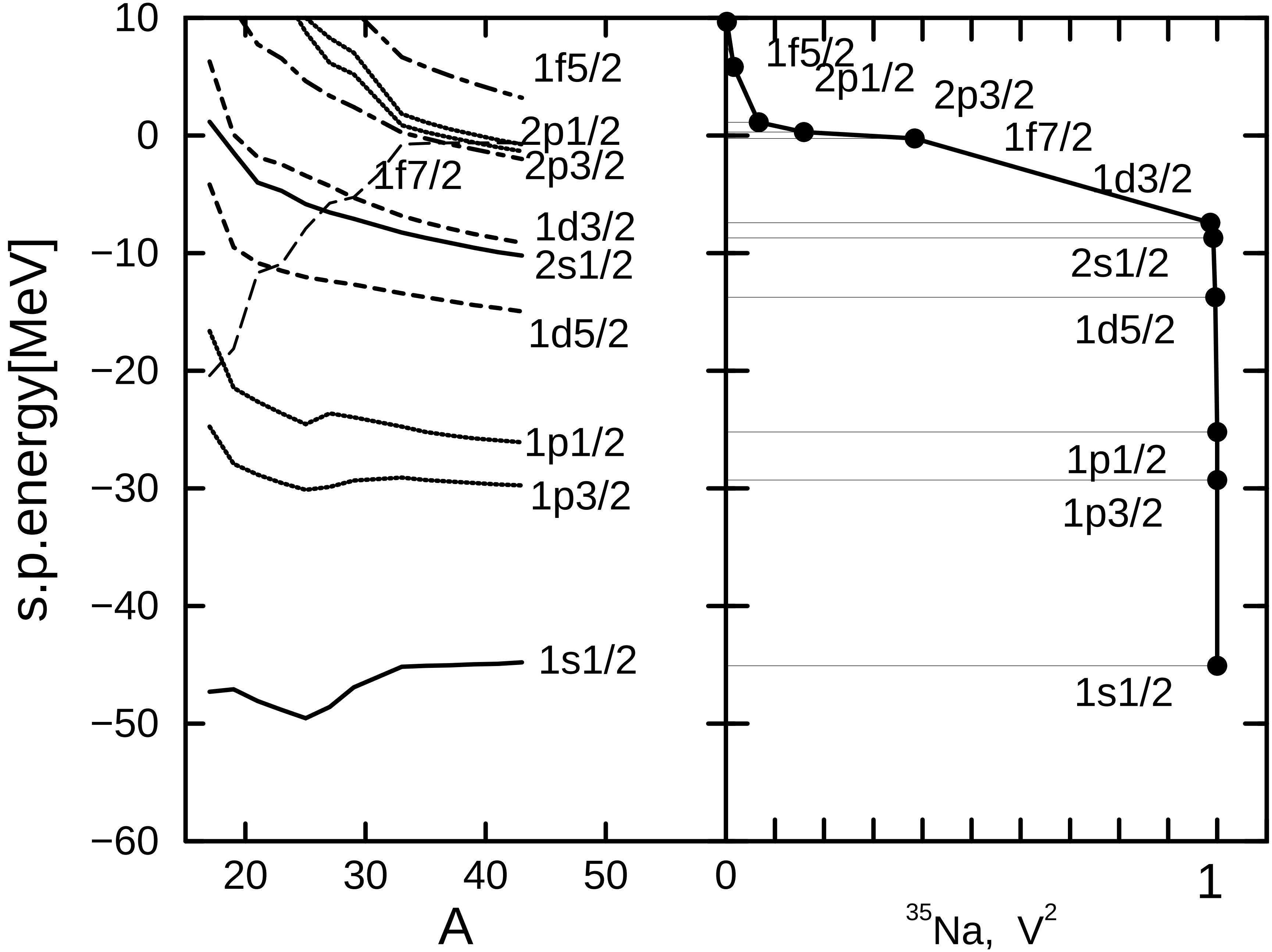

s.p.energy[MeV]
10
0
−10
−20
−30
−40
−50
−60
20
30
40
50
A
1f5/2
2p1/2
2p3/2
1f7/2
1d3/2
2s1/2
1d5/2
1p1/2
1p3/2
1s1/2
0
1
35Na, V2
1f5/2
2p1/2
2p3/2
1f7/2
1d3/2
2s1/2
1d5/2
1p1/2
1p3/2
1s1/2